

# X-Dimensional Display: Superimposing 2D Cross-Sectional Image inside 3D Wireframe Aerial Image

Y. Furuyama<sup>1</sup>, Y. Makino<sup>1</sup> and H. Shinoda<sup>1</sup>

<sup>1</sup>The University of Tokyo

---

## Abstract

*In this paper, we propose a new interactive volumetric display which simultaneously shows a floating 3D image and its 2D cross sectional image inside it. This display enables users to see an arbitrary cross sectional image by inserting a hand-held semi-transparent screen into the 3D image floating in the mid-air. This system has following possibilities: doctors easily see MRI images inside the 3D body image, and designers check the internal structure of a 3D object in CAD. We construct a prototype device to demonstrate our proposed method by combining a 3D display and an aerial imaging technology. The spinning LED array constructs the volumetric image, and which is optically mirrored to appear in the free-space by the transmissive mirror called Aerial Imaging Plate (AIP). We find that a fine meshed silk screen can be inserted into the aerial image without disturbing the shape of it. Cross sectional images can be projected onto it together with the 3D image. We demonstrate how a silk screen diffuses a 3D aerial image and a projected 2D image.*

Categories and Subject Descriptors (according to ACM CCS): I.3.3 [Computer Graphics]: Display algorithm.

---

## 1. Introduction

In this paper, we propose a new display system which constructs an aerial three-dimensional (3D) wireframe image and a two-dimensional (2D) image superimposed inside it at the same time. This system renders a 3D image in the air, and then projects a 2D image on a semi-transparent screen which is inserted into the 3D image. Our technique allows users to slice a wireframe image by intuitively inserting a screen into a 3D image to see its sliced cross-sectional image.

The cross-sectional images of 3D objects are used in several fields such as MRI images in a medical field, 3D design works, and numerical simulations of physics. Currently, users select a certain cross-sectional plane by inputting its coordinate values or moving the section with a mouse. There are some researches that enable users to slice a 3D image intuitively. VolumeSlicingDisplay [CI09] renders 2D cross-sectional images corresponding to the posture of the 2D screen device held by a user. Users can see sequential 2D images by moving the screen device. In this system, sometimes it is difficult to search the exact plane since users cannot find the 3D position to be sliced. Moreover, it is also difficult to imagine the whole shape and size of the 3D object by using the sets of 2D cross-section images. In contrast,

our system renders both the 3D wireframe and 2D cross-sectional image on the same physical coordinates. The advantage of our display is that users can find a particular cross-sectional image using a 3D wireframe as a hint for determining a slicing location.

To achieve our purpose, we construct an interactive 3D display combining a 3D display of rotating 2D LED array and an aerial imaging technology. First, rotating 64 x 64 LEDs create a light pattern in 3D space based on a persistence of vision. Since interaction with this 3D image by fingers or any tools is impossible due to the rotating mechanical parts, we use the special transmissive mirror: the Aerial Imaging Plate (AIP) [Asu11] manufactured by Asukanet Co. Ltd. This mirror is composed of many tiny cornered mirrors. The AIP optically reconstructs the touchable aerial image of a real object which is set at the other side of the AIP. Details are given in 3.1.

We superimpose a cross-sectional image inside the 3D floating image by using a semi-transparent screen and a projector. We use a fine mesh screen called a silk screen as a semi-transparent projection screen. The silk screen put inside the 3D aerial image does not diffuse its shape since light rays can pass through the small mesh of the screen to form the 3D image. Combining the screen posture detection and the rear-projection, we realize a new display system which

enables us to view the cross sectional 2D image in the 3D image simultaneously.

Our 3D display has about 9000 voxels with its refresh rate of 15.5 Hz. By calibrating the floating image position with projector's coordinate, the 3D display with high precision but low resolution is easily created and controlled. Many other research have developed higher resolution 3D displays than ours. We can easily replace our rotating display with those high-quality 3D displays. Details of the other 3D displays are described in next section.

## 2. Related works

3D image display systems are roughly categorized into three types. The first one is to display two different 2D images to each eye with parallax. Observers feel depth of the image based on the parallax. Some of them have used polarization filtered glasses, Head-Mounted Display (HMD) [Sut68] and so on. In these cases, users have to wear a device on them. Some of them have used special equipment on the display surface such as a lenticular lens, parallax barriers [KOS\*01], and Fresnel lens [UIS\*14]. In these methods, users have to see the display within an appropriate viewing angle.

The second one is to create light distribution pattern in the mid-air. Some of them have used small floating objects to project image on them such as fog screen [Fog02] [Hel01] and small particles trapped by ultrasound [OTR14]. Others have utilized the persistence of vision. A rotating LED array or a rotating projection screen produces 3D volumetric images [JK84] [KOF9393] [LBB\*02]. Laser induced plasma is another method to add light source in the air [KUY06].

The third one is to reconstruct light field. A famous example is holography, which records and reconstructs phase information of light waves as well as its intensity [sHBL\*90] [HMK91]. A concave mirror can also be used to reproduce light field in the air [BHI\*11]. Projection on a rotating mirror creates a light field [JMY\*07]. Recently a novel optical device: AIP has been proposed [Asu11]. The AIP is composed of tiny mirrors and reproduces an object image in mid-air (details are given in next section). There is a similar light field reconstruction method based on retro-reflective material [YS13].

In this paper, we combine the second and the third principles. A rotating volumetric display observed via the AIP presents 3D volumetric floating image in the mid-air.

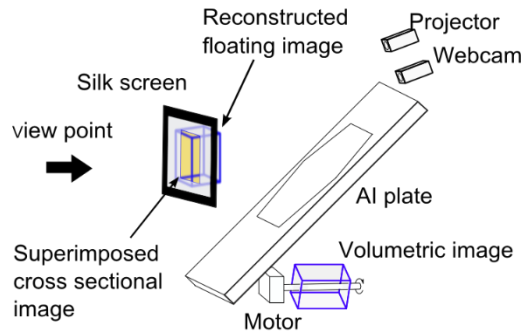


Figure 1: System configuration.

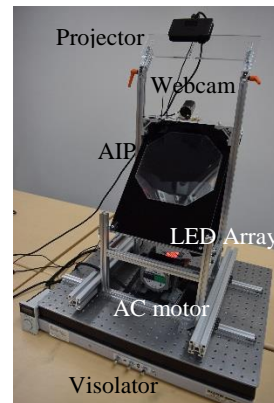


Figure 2: Prototype device.

## 3. System Configuration

We show our system configuration in Figure 1 and the prototyped device in Figure 2. This system is composed of the volumetric display, the AIP to reconstruct the image in the mid-air, the silk screen to be projected cross sectional images on it, the webcam to detect the screen location, and the projector.

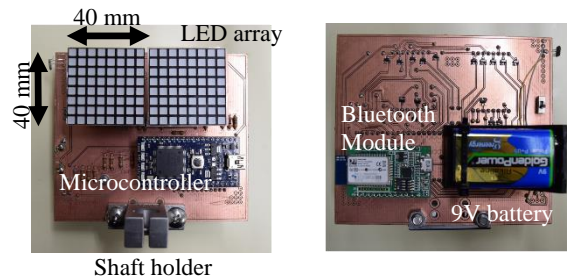


Figure 3: 3D Volumetric Display. (Left)Top view. (Right)Bottom view.

### 3.1 3D Volumetric Display

Figure 3 shows the 3D volumetric display. The spinning LED array constructs a volumetric image based on persistence of vision. Two sets of 64-LEDs arrays mounted bilaterally symmetrically on the AC motor shaft (BLM5120-A2,

Oriental Motor) which rotates at 930 rpm. Each LED is controlled by the microcontroller (LPC1768, NXP) corresponding to the rotation angle at intervals of every 2.5 degrees (144 steps in total). This display can generate 9216 voxels image in the cylindrical area whose radius is 4 cm and height is 4 cm and its volumetric refresh rate is 15.5 Hz. 3D light patterns are sent from PC via Bluetooth communication.

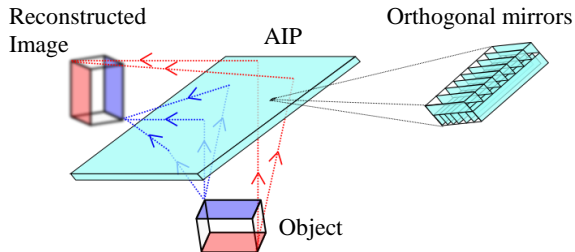


Figure 4: Aerial Imaging Plate.

### 3.2 Aerial Imaging Plate

The Aerial Imaging Plate (AIP) is a commercially-available optical device that reconstructs light patterns in the air. The basic principle of the AIP is shown in Figure 4. Orthogonal tiny mirrors are arrayed two dimensionally. When the AIP is tilted 45 degrees from the horizontal plane, where an object locates, a floating image of it appears before the AIP. This image is viewable without using any special glasses. We use an octagonal shape of the AIP, 10 cm each side, which is located 30 cm above the spinning volumetric display. In this configuration, the 3D image floats 20 cm before the AIP.

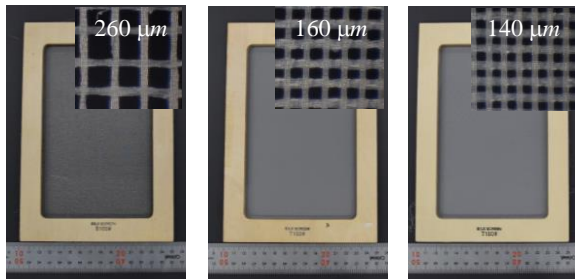


Figure 5: The whole views and closeups of the three types of silk screens. (Left) T100 whose mesh interval is 260  $\mu\text{m}$ . (Center) T150 whose mesh interval is 160  $\mu\text{m}$ . (Right) T180 whose mesh interval is 140  $\mu\text{m}$ .

### 3.3 Silk Screen

We used a silk screen as a semi-transparent projection screen which consisted of densely knitted fibers shown in Figure 5. We tried to understand the effect of the screen insertion. We used different mesh pitch silk screens whose intervals of 140, 160, and 260  $\mu\text{m}$ , respectively. Since the size

of the mesh is large enough compared to the light wavelength, the effect of the diffraction is small. The main effect of the insertion of a silk screen is occlusion and diffusion at the silk string. The light rays mainly go through small meshes keeping its directional information, therefore a volumetric image is reconstructed even when the silk screen is inserted into the image. We evaluated this effect in section 5.

### 3.4 Camera and Rear-projector

The position and orientation of a silk screen is estimated by using a webcam. Four markers located on each corner of the silk screen is captured by the webcam and processed by OpenCV library. A cross-sectional image is calculated based on the position and orientation of the screen and rendered onto the silk screen using OpenGL. The image is projected from the projector (PK320, Optoma) set above the AIP as shown in Figure 2.

## 4. Performance of the proposed system

### 4.1 3D wireframe image

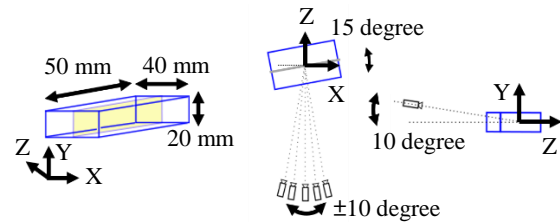
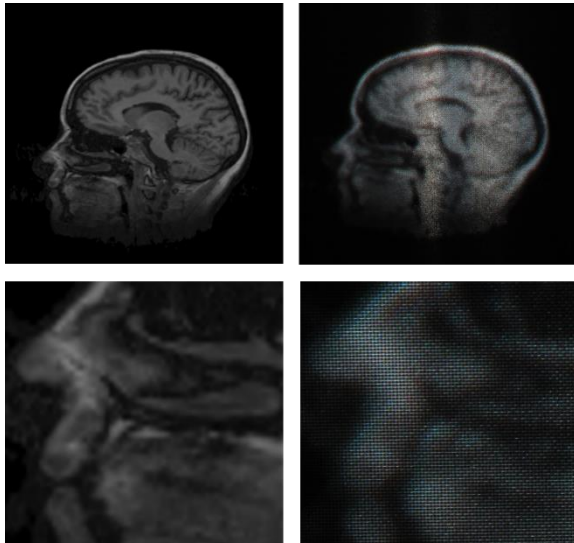


Figure 6: The demonstration setup. (Left) Constructed 3D cuboid blue image. The silk screen was located as it sliced the yellow region. (Center) Camera setup from top view. (Right) Camera setup from right view.

We show the performance of our prototype. Figure 6 (Left) shows a 3D cuboid model, we prepared as a sample 3D wireframe, whose size is 50 mm in width, 40 mm in depth, and 20 mm in height and rotated 15 degrees around the Y-axis. Figure 8 shows the aerial images by our system, captured in setup shown in Figure 6 (Center and Right). These captured images are changed according to the view angles.

Figure 9 shows the 3D images passing through the T180 silk screen which is located to slice the 3D image shown in Figure 6 (Left). Each LED point is blurred and its intensity is weakened by the insertion of the screen, however the whole shape of the 3D image is clearly kept.



**Figure 7:** Projected brain image. (Left) Raw image. (Right) Projected image on the T180 silk screen. (Bottom) Zoomed image.

#### 4.2 2D projection image

Figure 7 shows the 40 x 40 mm image of the cross-sectional human brain image projected on the silk screen. No volumetric image is superimposed in this case. The resolution of the projected image on the silk screen depends on both the mesh pitch of the screen and the projector performance. Since the silk screen has small holes the projected image is seen as a meshed image when zoomed (Figure 7 bottom-right). However, each hole size is several hundred  $\mu\text{m}$  and the details of the brain image is sufficiently visible.

#### 4.3 2D projection image superimposed inside the 3D image

Figure 10 shows the cross-sectional 2D image projected in the cuboid wireframe. The 2D projection image and the 3D image are simultaneously visible. 3D wireframe beyond the 2D projection image is also visible.

The Figure 11 shows another example of our display. We constructed a 3D model of a human head facing left, whose size is 30 mm in width, 30 mm in depth, and 40 mm in height. Same as the cuboid example, it appears that the 3D image kept its shape when the silk screen is inserted into it, and the cross-sectional brain image coexisted with the 3D wireframe image.



**Figure 8:** The 3D cuboid wireframe image (50 mm in width, 40 mm in depth, and 20 mm in height and rotated 15 degrees around Y-axis shown in Figure 6.) (Left) View from 10 degree left. (Center left) View from 5 degree left. (Center) View from the center. (Center right) View from 5 degree right (Right) View from 10 degree right.



**Figure 9:** The 3D image that the silk screen was located as it sliced the yellow region in Figure 6.



**Figure 10:** The 3D image and its 2D cross-sectional image projected on the silk screen.





**Figure 11:** The 3D human head model image and its 2D cross-sectional image projected on the silk screen. (Left) 3D human model image composed of a cuboid, a leftward arrow, and a pentagon. (Center Left) Constructed 3D wireframe image from front view. (Center) A 3D image in which the silk screen is inserted. (Center Right) Superimposed 2D cross-sectional blue image of the wireframe. (Right) Superimposed 2D brain image inside the 3D head image.

## 5. Basic Experiment

### 5.1 Experiment 1: Evaluation of the 3D aerial image and 2D projection image

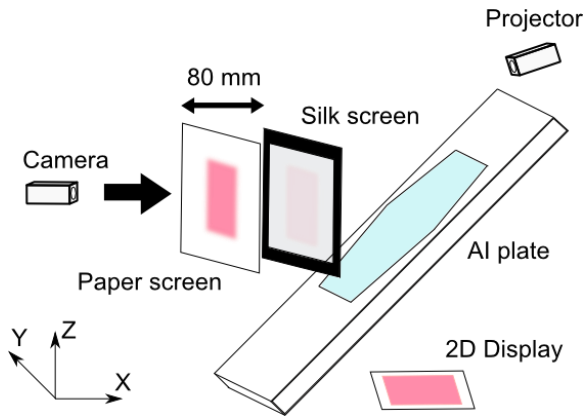


**Figure 12:** Experiment 1 Setup.

#### 5.1.1 Method

We conducted the experiment to evaluate the effect of the insertion of a silk screen. We evaluated 2 points, how an aerial image was diffused by the silk screen and how clear the projected image was on the silk screen.

The experimental setup is shown in Figure 12. We used a 2D red-squared image on LCD as a light source of the aerial image. A paper was used for projecting the red square at the focal location, parallel to YZ plane. The silk screen was inserted between the paper screen and the AIP. The insertion of the silk screen can disturb the clarity of the red square image on the paper screen. We captured the edge region of the red square image on the paper screen by 20.0  $\mu\text{m}/\text{pixel}$  while changing the silk screen pitch (i.e. T100, T150, T180 and without a silk screen). We calculated the  $x$ -directional image intensity and its power spectrum from

$$I(x) = \sum_y H(x, y) \quad (1)$$

$$P(u) = FFT[I(x)] \quad (2)$$

where  $H(x, y)$  is a pixel value at  $(x, y)$  and  $u$  is a spatial frequency along  $x$  axis.

Then, we projected a plain red image onto the silk screen to evaluate how the silk screen can be used as a projection surface. When the mesh interval is large the projected image becomes rough and dark. We captured the image on the silk screen at 20.0  $\mu\text{m}/\text{pixel}$  and calculate its  $x$ -dimensional power spectra from the equation (2).

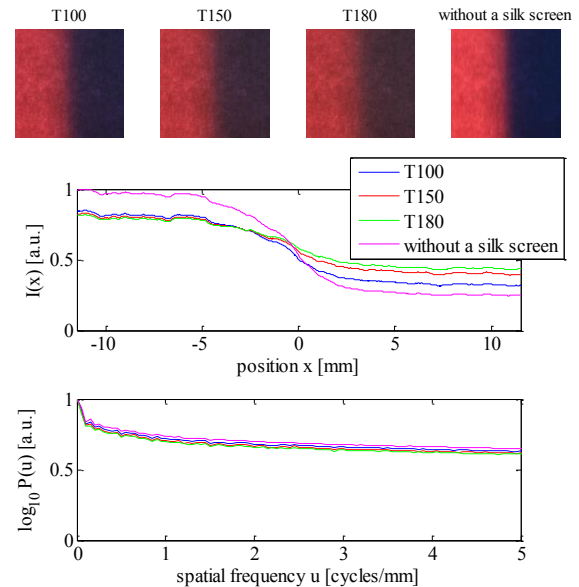


**Figure 13:** The mesh pitch effects on aerial image. (Top) Captured images. (Middle) The  $x$ -directional pixel value. (Bottom) Logarithm power spectra.

#### 5.1.2 Result

Aerial images on the paper screen and their logarithm power spectra are shown in Figure 13. Compared to the result of “without a silk screen” condition, the aerial image is blurred by the insertion of the silk screen. It also suppresses the light intensity. The finer silk screen blurs the edge of the aerial image more. The change of the pitch of the silk screen does not affect to averaged light intensities.

Projected plain images on the silk screen and their logarithm power spectra are shown in Figure 14. As shown in the raw data, the projected image is affected by the mesh pitch. The peak power of the spectra is found at the spatial frequency corresponding to the each mesh pitch. The projected image on the fine mesh silk screen is clear and sharp. These results suggests the fine mesh screen suits for 2D image projection, though it does not appropriate for keeping shape of the 3D image.

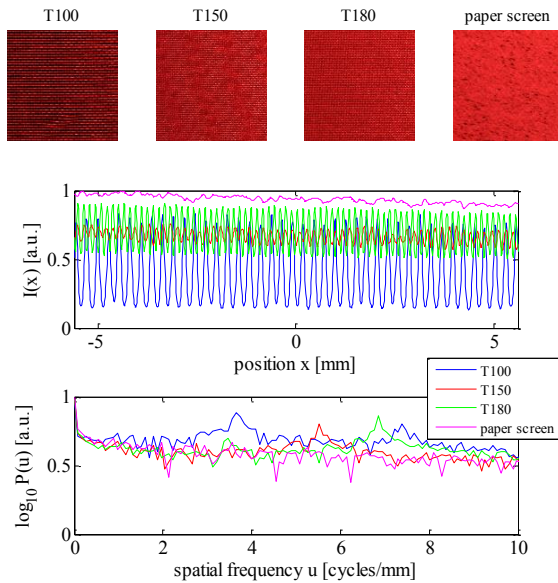


**Figure 14:** The mesh pitch effects on the projection image. (Top) Captured image. (Middle) The x-directional pixel value. (Bottom) Logarithm power spectra.

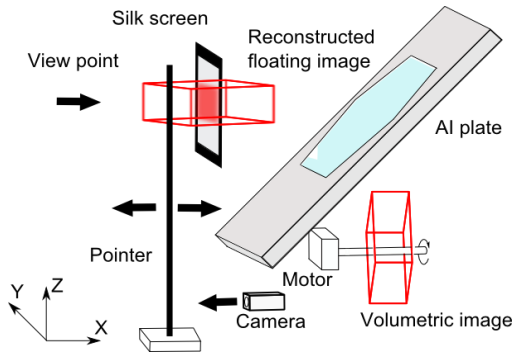


**Figure 15:** Experiment 2 setup.

## 5.2 Experiment 2: User study

### 5.2.1 Method

The purpose of this experiment is to demonstrate that users can see the volumetric floating image as 3 dimensional even when a silk screen is inserted. To achieve our concept,

the depth of the low resolution wireframe image must be recognized as 3D. Additionally, The fine meshed silk screen must not block the 3D image. Since the diffusion of the 3D image depends on both the mesh pitch and slicing location, we evaluate the user perception while changing these conditions.

The experimental setup is shown in Figure 15. This experiment is conducted in following procedure. Eight subjects stood in front of our device. They closed their eyes as an initial condition. A silk screen is inserted inside the aerial cuboid wireframe image (6 cm in width, 6 cm in depth, and 2 cm in height) parallel to the YZ plane as shown in Figure 15. Then, they were asked to open their eyes and to move the pointer along X axis to indicate the nearest position of the 3D image. The difference between the pointer location and the true one is measured by the camera. This sequence is repeated while changing the silk screen conditions. We changed two parameters: two screen positions (at the middle and the behind of the 3D cuboid image) and two screen pitches (T100 and T180). For comparison, we also experimented in no silk screen condition. Thus there were 5 conditions: 2 positions  $\times$  2 pitches + no screen. Each condition was repeated 5 times in random order. In total, 25 trials were conducted to one subject. Eight male examinees, whose ages were 20-25 years old, participated in this experiment.

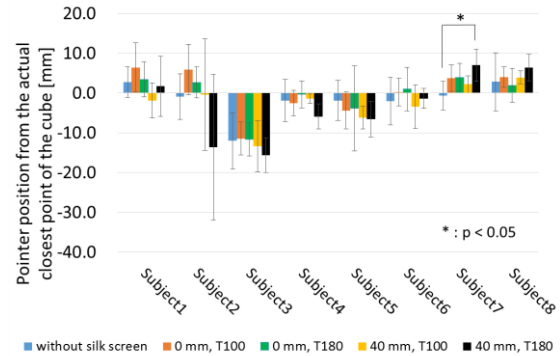


**Figure 16:** The mean distance between pointer location and actual one. Error bar means a standard deviation.

### 5.2.2 Result

The result is shown in Figure 16. Each bar represents the mean distance between the indicated position and the actual one. The positive value means that examinee set the pointer nearer to their view point. Each error bar means the standard deviation. T-tests are conducted between the result of without a silk screen and other 4 conditions. There were no significant differences among the most results between with/without a silk screen except for Subject 7. Most examinees located the pointer within 10 mm from the actual position. Thus, users can see the aerial image as 3D. The insertion of the silk screen does not affect to the 3D shape recognition.

In this experiment, we receive many qualitative comments from examinees. Some felt easy to recognize the 3D

shape and some did not. One examinee could not perceive the depth of the 3D image when he approached to the 3D image. He said the viewing distance was important to recognize 3D structure. This comment suggests the view point is important.

## 6. Limitations

We discuss the limitations about 3D volumetric display and the AIP.

### 6.1 3D Volumetric Display

The spatio-temporal resolution of the rotating volumetric display depends on the resolution and refresh rate of the screen and its rotating speed. The resolution of our volumetric display is 9216 voxels and the volumetric refresh rate is 15 Hz. We construct this prototype to show the basic principle of our concept. Our system can be easily combined with another high resolution 3D display and we have to choose the appropriate one depending on the requirement.

### 6.2 Aerial Imaging Plate

The AIP is composed of an array of tiny corner reflectors. The array pitch defines the resolution of reconstructed aerial images. Currently the interval of the mirrors is about 0.5 mm. For achieving fine volumetric images, higher resolution version of the AIP is desirable, though the current AIP has sufficiently high spatial resolutions.

The visible position of the 3D virtual image depends on the sizes of the AIP and the reconstructed objects. The virtual image appeared 15.5 cm from the plate in this time. Assuming that the size of the object is about 5 cm, the visible angle will be about  $\pm 16$  degrees when we used the AIP of 23.5 cm square. To realize wider visible range, the AIP should be larger.

### 6.3 Necessity of 2D projection

When we assume an ideal high-resolution 3D volumetric display, we do not need to have a projector for projecting 2D image. The ideal 3D display can show both the 3D image and its cross-sectional image at the same time.

We used a projector in the current study because there is no such high-resolution 3D display yet. For example, Jones et al. realized the high-quality 3D display [JMY\*07] that has 768 x 768 voxels updated by 20 Hz. They demonstrated high quality 3D volumetric images. In contrast, a commercially available small projector allows 1280 x 800 resolution 2D images with 60 fps. In order to achieve high resolution and interactive 2D image superimposed into the 3D image, we thought it was better to use a projector. The situation can be changed depending on the development of 3D displays.

## 7. Applications

Our system can superimpose a 2D image onto a 3D volumetric image. This enables users to interact with 2D and 3D images at the same coordinates. The main application of this

interaction is intuitive handling of 3D CAD data. Usually people see 3D CAD data by projecting it onto a 2D plane such as elevation, bird's-eye, and cross section views. Sometimes it is difficult to set those cross section planes intuitively. Our method allows users to insert a cross section plane at arbitrary location and angles. This visualizing method will be useful for comprehending 3D analytical results of structures, fluids behaviors, electromagnetic fields and so on.

This technology also can be applied for a medical field. Currently, medical doctors measure 3D information of human body with the MRI or some other visualizing technologies. Although such data is usually presented on a conventional 2D display, our system allows doctors to see both 3D and 2D images at the same time. They can observe arbitrary cross section images intuitively. Our system would be one of the useful interfaces for those purposes.

## 8. Conclusion

In this paper we proposed a novel volumetric display that can superimpose 2D images inside it. We used two key technologies: a rotating volumetric display and the Aerial Imaging Plate (AIP). Combination of these technologies produces interactive volumetric images in the air. Images can be seen as 3D even when a semi-transparent silk screen is inserted into it. Thus users can interact with volumetric images superimposing their cross sectional images by projecting it on the silk screen. In this paper we demonstrated a basic configuration of the system and experimentally showed that the insertion of the silk screen did not affect to the perception of 3D image. Examinees could point out a nearest point of a produced 3D image independent on the insertion of the silk screen. This technology can be used for manipulating 3D data intuitively such as MRI images in medical field.

## Reference

- [Asu11] ASUKANET CO. LTD: AI PLATE (2011)  
<http://aerialimaging.tv/index.php>
- [BHI\*11] BUTLER, A., HILLIGES, O., IZADI, S., HODGES, S., MOLYNEAUX, D., KIM, D., AND KONG, D.: Vermeer: direct interaction with a 360° viewable 3D display. *In Proceedings of the 24th annual ACM symposium on User interface software and technology (2011)*, New York, NY, USA, 569-576.
- [CI09] CASSINELLI, A., AND ISHIKAWA M.: Volume Slicing Display, *SIGGRAPH ASIA '09 (2009)*, *Emerging Technologies*
- [Fog02] FOGSCREEN (2002)  
<http://www.fogscreen.com/>
- [Hel01] HELIODISPLAY (2001)  
<http://www.io2technology.com/>
- [HMK91] HASHIMOTO, N., MOROKAWA, S., AND

- KITAMURA K.: Real-time holography using the high-resolution LCTV-SLM, *Proc. SPIE 1461, Practical Holography V*, 291 (1991).
- [IHT08] IZADI, S., HODGES, S., TAYLOR, S., ROSENFELD, D., VILLAR, N., BUTLER, A., AND WESTHUES J.: Going Beyond the Display: A Surface Technology with an Electronically Switchable Diffuser, In *Proceedings of the 21st annual ACM symposium on User interface software and technology (UIST'08)* (2008), 269-278.
- [JK84] JANSSON, D. G. AND KOSOWSKY R. P.: Display of Moving Volumetric Images", *Proc. SPIE 0507, Processing and Display of Three-Dimensional Data II*, 82 (1984).
- [JMY\*07] JONES, A., MCDOWALL, I., YAMADA, H., BOLAS, M., AND DEBEVEC, P.: Rendering for an interactive 360° light field display. In *ACM SIGGRAPH 2007 papers* (2007), New York, NY, USA, Article 40.
- [KOF93] KAMEYAMA, K., OHTOMI, K., AND FUKUI, Y.: Interactive 3-D Volume Scanning Display with Optical Relay System and Multi-Dimensional Input Device, *Stereoscopic Displays and Applications IV, vol. 1905* (1993).
- [KOS\*01] KUNITA, Y., OGAWA, N., SAKUMA, A., INAMI, M., MAEDA, T. AND TACHI, S.: Immersive Autostereoscopic Display for Mutual Telexistence: TWISTER I (Telexistence Wide-angle Immersive STEReoscope model I). In *Proceedings of IEEE VR 2001*, 31-36.
- [KUY06] KIMURA, H., UCHIYAMA, T., AND YOSHIKAWA, H.: Laser produced 3D display in the air. In *Proceedings of ACM SIGGRAPH 2006 Emerging Technologies* (2006).
- [LBB\*02] LANGHANS, K., BAHR, D., BEZECNY, D., HOMANN, D., OLTMANN, K., OLTMANN, K., GUILL, C., RIEPER, E., AND ARDEY, G.: FELIX 3D display: an interactive tool for volumetric imaging, *Proc. SPIE 4660, Stereoscopic Displays and Virtual Reality Systems IX*, 176 (2002).
- [OTR14] OCHIAI, Y., TAKAYUKI, H., AND REKIMOTO, J.: Pixie dust: graphics generated by levitated and animated objects in computational acoustic-potential field. *ACM Trans. Graph.* 33, 4, Article 85 (July 2014), 13 pages.
- [SHBL\*90] ST-HILAIRE, P., BENTON, S. A., LUCENTE, M. E., JEPSEN, M. L., KOLLIN, J., YOSHIKAWA, H., AND UNDERKOFFLER J. S.: Electronic display system for computational holography, *Proc. SPIE 1212, Practical Holography IV*, 174 (1990).
- [Sut68] SUTHERLAND, I. E.: A head-mounted three dimensional display. In *Proceedings of the December 9-11, 1968, fall joint computer conference, part I (AFIPS '68 (Fall, part I))*, 757-764.
- [UIS\*14] UEDA, Y., IWAZAKI, K., SHIBASAKI, M., MIZUSHINA, Y., FURUKAWA, M., NII, H., MINAMIZAWA, K., AND TACHI, S.: HaptoMIRAGE: mid-air autostereoscopic display for seamless interaction with mixed reality environments. In *ACM SIGGRAPH 2014 Emerging Technologies*
- [YS13] YAMAMOTO, H., AND SUYAMA, S.: Aerial Imaging by Retro-Reflection (AIRR). *SID Symposium Digest of Technical Papers* (2013), Vol.44, No.1, pp.895-897.